# Hybrid Turbocharging for Alternatively Fueled Internal Combustion Engines in Naval Applications

Vollbrandt, J.; Coraddu, A.; Geertsma, R. D.

**Important note**
To cite this publication, please use the final published version (if applicable).
Please check the document version above.

# Hybrid Turbocharging for Alternatively Fueled Internal Combustion Engines in Naval Applications

Ir. J Vollbrandt[a,b*], Dr. A Coraddu, MSc, CEng, MIMarEST[a], Dr. ir. R D Geertsma, CEng, FIMarEST[a,b]

[a]*Delft University of Technology, The Netherlands;* [b]*Netherlands Defence Academy, The Netherlands*

*Corresponding author. Email: j.vollbrandt@tudelft.nl

**Synopsis**

The global shipping industry is at a crucial juncture, facing an urgent need to reduce greenhouse gas emissions in the short to medium term to mitigate climate change. A shift towards alternative fuels is imminent, necessitated by the limitations in current fuel cell and battery technology in terms of power density. Addressing this, navies worldwide are not only exploring the use of alternative fuels to diminish environmental impact but also seeking solutions to reduce emissions signatures and decrease reliance on fossil fuels. In this paper, we investigate the use of hybrid turbocharging to improve the dynamic performance of alternatively fueled combustion engines. We extended an existing and validated Mean Value First Principle (MVFP) engine model of a spark-ignited (SI) throttle-controlled Caterpillar 3508*A* gas engine with a hybrid turbocharger. The study investigates the impact of electrical power Power-Take-In/Off from the turbocharger shaft on the engine's air path dynamics for different use cases, considering transient and steady state phases. We demonstrate that a generator set can benefit from hybrid turbocharger by significantly reducing the engine speed drop and settling time after a load step. While accelerating from 0 to cruise speed, propulsion engines benefit less from hybrid turbocharger, due to risk of compressor surge during low engine speeds. The overall results show that simply adding electric power to the turbocharger shaft during transient phases does not unlock the full potential of hybrid turbocharging for alternatively fueled combustion engines. The implementation of hybrid turbocharging requires careful integration, reconsideration of sizing and matching of turbine and compressor, and the combination with blow-off, blow-by, and waste gate valves to prevent compressor surge. However, the capability for electrical power take-off/in within a larger propulsion and electrical power generation plant context suggests a reduction in spinning reserves and an increase in overall system efficiency during steady state. Thus, implementing hybrid turbocharging can play an important role in the transition to alternative fuels and the reduction of greenhouse gas emissions.

*Keywords:* Modeling and simulation; Mean value first principle model; Transient performance; Alternative fuels; Hybrid Turbocharging

## 1 Introduction

Current fuel-cell and battery technology cannot provide sufficient energy and power density for naval vessels in the short and medium term [38, 29, 32]. Therefore, navies worldwide investigate the use of alternative fuels in combustion engines to reduce greenhouse gas emissions, reduce signatures, and lessen their reliance on fossil fuels. While gas turbines are still considered for providing boost power to naval combatants due to its high power density, the majority of naval vessels rely on fuel-efficient turbocharged diesel engines to sail at cruise speed [9, 12, 57, 49]. Alternative fuels that can replace F76 in these conventional propulsion systems are consequently favoured.

Since its introduction more than a century ago, turbocharging is probably the most important driver of increasing fuel efficiency and power density of the diesel engine [56, 27]. The majority of modern marine four stroke engines adopt a single-stage charging concept due to its reliability and cost-efficiency. In these engines, the turbocharger delivers maximum charge pressure close to the point of nominal power for the highest power output and engine efficiency. However, in part-load operation of the engine, the turbocharger cannot maintain the maximum charge air pressure due to the reduced exhaust mass and energy flow. Consequently, the maximum engine torque and efficiency decrease accordingly [27, 4]. Various charging concepts, such as sequential and 2-stage turbocharging, have been developed to cope with deteriorating part-load performance [26, 28, 45, 34, 36], varying in complexity, maintainability, costs, and dynamic performance. However, so far, these concepts have only been adopted in niche applications, such as naval vessels, fast ferries and yachts [25, 60, 59, 5]. An alternative method of improving part load performance of single-staged turbocharged marine diesel engines is by

implementing hybrid turbocharging [58, 39]. Hybrid turbocharging has been researched extensively for automotive applications [30, 14, 43, 19] and is also referred to as e-turbocharging, next to possible configurations of electrical turbo-compounding and e-boosting [23, 31, 1]. E-turbocharging and electrical turbo-compounding have been applied first in high-performance engines, for example, in F1 racing [51, 6, 44], but can be found in road-going automotive engines by now [24, 17, 50]. Diesel engines for heavy-duty road transport have been developed with mechanical turbo-compounding [37, 55], but e-turbocharging will likely make its introduction in the next generation of heavy-duty CI engines [35, 8]. Investigating hybrid turbocharging for naval applications can combine two advantages: it can decrease fuel consumption [10, 46] and increase dynamic performance [62, 33].

For marine diesel engines, hybrid turbocharging has been examined to improve part-load efficiency and decrease engine fouling [52, 10, 11] or increase the efficiency of Selective Catalytic Reduction (SCR)-systems [42] on low loads during extensive phases of slow steaming. More interestingly is the implementation of hybrid turbocharging on marine internal combustion engines running on alternative fuels, for example, for large dual-fuel gas engines [20, 3, 40, 2]). By investigating steady-state operating conditions, the authors concluded that hybrid turbocharging systems can increase engine efficiency over the complete engine envelope, especially during gas-mode and under part-load conditions. During steady-state operations, two different cases need to be distinguished: withdrawal of electrical power from the turbocharger shaft, which we refer to as $PTO$, or Power-Take-Off, and addition of electrical power to the turbocharger shaft, which we refer to as $PTI$, or Power-Take-In.

With $PTO$, electrical power withdrawn from the turbocharger shaft is fed into the ship's electrical grid, ideally reducing the necessary amount of running auxiliary generators or the electrical power taken off via a shaft generator. In this case, the total system efficiency increases and might offset a decreasing main engine's efficiency due to a lower charge air pressure and resulting trapped mass, as discussed in [10, 20] A special case arises when the turbocharger is not matched to deliver maximum charge air pressure close to nominal power but at lower power output. Running at nominal power, a part of the charge air mass flow is discharged via a blow-off valve to prevent excessive charge air pressures. This would allow for electrical power withdrawn from the turbocharger shaft without penalizing the engine's efficiency [3, 2, 11].

With $PTI$, the additional energy fed to the turbocharger results in the engine's higher charge air pressure, thus increasing its efficiency. The necessary electric power is withdrawn from the ship's grid and must be included in the total fuel consumption. Nevertheless, $PTI$ is favourable when the increase in engine efficiency offsets the electrical power requirements, which might be the case during low engine load [52, 40]. While improving the fuel efficiency is an important achievement in reducing global greenhouse gas emissions, limited research has been conducted on improving the dynamic performance of marine internal combustion engines using hybrid turbocharging.

By investigating a typical naval acceleration manoeuvre, Rusman [47] concluded that hybrid turbocharging could improve the dynamic performance of the investigated diesel engine and decrease the time required for the manoeuvre. Westhoeve [58] investigated several load steps and load ramps with different settings of a hybrid turbocharger. He concluded that increasing the charge-air pressure before the load increase can achieve the largest performance gain. However, this might result in very high air-excess ratios and significant gas-mode misfire. Mestemaker et al.[39] propose hybrid turbocharging for large four-stroke diesel engines used on dredging vessels to reduce turbo-lag during highly fluctuating dredging operations. By implementing hybrid turbocharging, the recovery time of the engine subjected to load steps can be reduced, but the maximum loading capacity is not increased. Additionally, the control system has to be set up carefully to prevent thermal overloading of the engine. Although current research is limited to compression ignition engines, either on diesel or dual-fuel, the benefits of hybrid turbocharging for marine internal combustion engines are revealed.

The aim of this paper is to investigate hybrid turbocharging for marine spark-ignited combustion engines running on alternative fuels. Spark-ignited engines are currently the only available engines suited to run on 100% methanol and might, therefore, play an important role in the transition to alternative fuels. As discussed in [54], the dynamic performance of marine spark-ignited combustion engines can be limited by the inertia of the turbocharger and might benefit from hybrid turbocharging. For this reason, this work considers a naval combatant as a use case, equipped with two 5 MW gas engines with hybrid turbocharging. We investigate a typical acceleration manoeuvre of the vessel and PTO/PTI options during steady state operation.

## 2 Theoretical Framework

The engine simulation model used to generate the results presented in this paper is a generic model of a marine high-speed, 4-stroke, spark-ignited gas engine with a single point of injection. The proposed mean value first principle engine model relies on the filling and emptying approach for the air and exhaust path dynamics and the 6-point Seiliger cycle for the closed in-cylinder process. The model has been derived from the model as presented in [54], and the gas path has been further simplified to reduce calibration efforts and computational costs. The current model uses just one volume element for the inlet receiver since the volumes of the air cooler and exhaust receivers are very small compared to the volume of the inlet receiver, see Figure 1. The air cooler and exhaust

receiver are implemented by a simple pressure- and temperature loss. Hybrid turbocharging is represented by an additional torque, as shown in Figure 1, and the load is represented by a simple propeller model for mechanical propulsion and by a lumped load for an electrical power system.
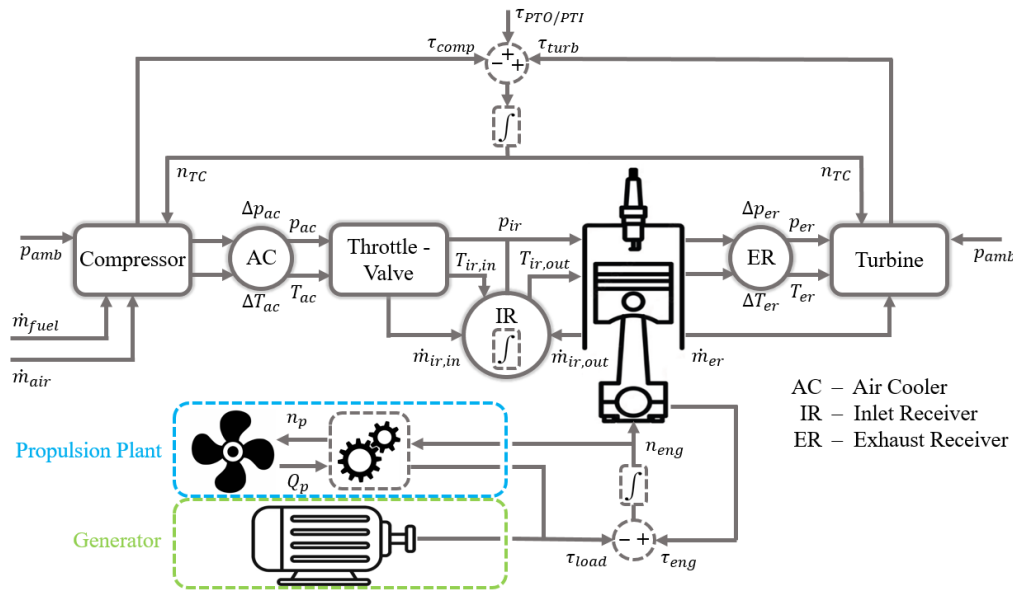


Figure 1: Block diagram of the proposed simulation model showing the reduction in volume elements involved in the gas exchange process and the investigated use cases with propulsion plant and generator.

### 2.1 Power take-off / Power take-in

With a hybrid turbocharger, PTO and PTI are realized by withdrawing and feeding electrical power with an electric motor/generator directly from the turbocharger shaft. For this research, the electric motor/generator is not modelled, but the corresponding torque is simply added or subtracted to the shaft. The turbocharger shaft speed is thus determined considering the following equation of motion:

$$\dot{n}_{TC} = \frac{1}{2\pi J_{TC}} \left( \eta_{m,TC}\tau_{turb} - \tau_{comp} + \tau_{PTO/PTI} \right), \tag{1}$$

with $n_{TC}$ the rotational speed of the turbocharger shaft, $\eta_{m,TC}$ the mechanical efficiency of the turbocharger, $\tau_{turb}$ the torque delivered by the turbine, $\tau_{comp}$ the torque requested by the compressor, $\tau_{PTO/PTI}$ the torque withdrawn or fed by the electric motor/generator and $J_{TC}$ the turbochargers mass moment of inertia.

### 2.2 Propeller and Hull Model

A propeller model is necessary to predict the delivered thrust force and the required torque from the engine based on the rotational speed of the shaft. Fast naval combatants with combined diesel $\vee$ gas (CODOG) / with combined diesel $\wedge$ gas (CODAG) propulsion plants are typically equipped with a controllable-pitch propeller (CPP). To predict propeller thrust, torque and efficiency, the open water test results of the Wageningen C-series [16, 15] have been implemented in the propeller model. To read out the four quadrant diagram, the hydrodynamic pitch angle $\beta$ is determined by:

$$\beta = \arctan\left(\frac{v_a}{0.7\pi n_p D_p}\right), \tag{2}$$

with $n_p$ the shaft speed, $D_p$ the propeller diameter, and $v_a$ the propeller advance speed, which is determined by:

$$v_a = v_s(1 - f_w), \tag{3}$$

with $v_s$ the ship speed, and $f_w$ the wake fraction. The four quadrant diagram provides the thrust coefficient $C_T$ torque coefficient $C_Q$ for the desired propeller pitch setting and are used to calculate propeller thrust $T_P$ and torque $Q_P$ via:

$$T_P = C_T \frac{1}{2}\rho v_h^2 \frac{\pi}{4} D_p^2 \tag{4}$$

$$Q_P = C_Q \frac{1}{2} \rho v_h^2 \frac{\pi}{4} D_p^3, \tag{5}$$

where $v_h$ is the hydrodynamic velocity and can be calculated via:

$$v_h = \sqrt{v_a^2 + (0.7 \pi n_p D_p)^2} \tag{6}$$

Due to the propeller's interaction with the hull, the requested torque of the propeller installed after the ship slightly deviates from the torque of an open-water propeller. Therefore, the relative rotative efficiency $\eta_r$ is introduced [61]:

$$\eta_r = \frac{Q_P}{M_P}, \tag{7}$$

where $M_P$ is the torque requested by the propeller behind the vessel. To account for the time delay between changing the propeller pitch set point and the actual movement of the propeller blades, Geertsma [21] proposes the following first-order linear equation:

$$\dot{PD} = \frac{1}{\tau_{PD}} (PD_{set} - PD), \tag{8}$$

with $PD(t)$ the actual pitch of the propeller, $PD_{set}(t)$ the pitch set point, and $\tau_{PD}$ representing the actuation delay. The hull model relates the thrust generated by the propellers to speed of the ship via the following equation of motion:

$$\dot{v}_s = \frac{1}{m_{ship}} \left[ k_p T_P - \frac{R_{ship}(v_s)}{1 - f_t} \right], \tag{9}$$

with $k_p$ the number of propellers, $R_{ship}$ the ship resistance as a function of the ship speed, $f_t$ the thrust deduction factor, and $m_{ship}$ the mass of the ship. The equation of motion limits the ship's dynamics to just one degree of freedom, in surge direction, which is considered to be sufficient for the analysis of acceleration manoeuvres.

### 2.3 Controller Model

The engine control model has been introduced in [54], see Figure 2. The engine speed is controlled by the throttle valve, forming a controllable restriction on the mass flow of gas from the compressor to the the inlet receiver. A PID controller generates setpoints for the throttle valve. A TecJet gas valve adjusts the fuel flow, controlling the amount of fuel added to the inlet air before the compressor. The TecJet's PID controller uses tabular values for the desired air-to-fuel ratio and the actual air-to-fuel ratio received from the inlet receiver conditions.

## 3 Case Study

The Caterpillar 3508A high-speed, 4-stroke, spark-ignited gas engine is used for the case study. This engine is currently running on natural gas from the grid but has run on methanol and different blends of NG with hydrogen in the past [48, 7] and is, therefore, a suitable representative for a marine spark-ignited engine able to run on alternative fuels. The engine is presently used in the engine research facilities of the Netherlands Defense Academy in Den Helder. The test set-up and data acquisition are described in [54], and engine parameters are given in Table 1.
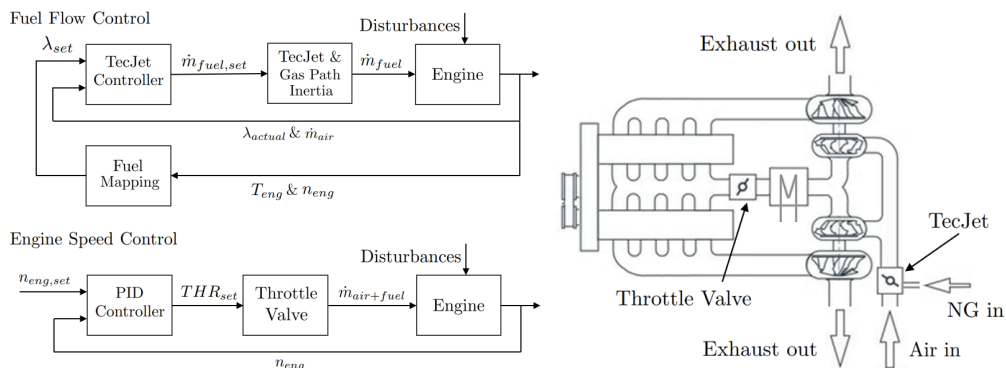


Figure 2: Schematic layout of the engine and controller from [54]

Table 1: Engine parameters Caterpillar 3508B

| Feature | Value |
| --- | --- |
| Number of cylinders | 8 |
| Rated speed | 1500 rpm |
| Cylinder arrangement | 60° V |
| Rated power | 500 kWe |
| Bore | 170 mm |
| Turbocharger type | Garrett TW6146 |
| Stroke | 190 mm |
| TC quantity | 2 |
| Displacement | 34.5 L |
| TC configuration | Parallel |
| Compression ratio | 12:1 |
| Max boost pressure | 2.25 bar absolute |
| Fuel type | Low-calorific natural gas |
| Injection method | Single point injection before TC |
| Ignition method | Spark ignited (SI) |

### 3.1 Validation Engine Model

For validation of the derived engine model, a measurement run on the experimental set up has been executed on constant engine speed with load steps increasing from 16% to 30%, 60%, and 80% and decreasing from 80% to 50% and 20% of the Maximum Continuous Rating (MCR) load. The validation run has been divided into segments with steady state operating points and dynamic segments with the transition between steady state operating points, as reported in Figure 3. To determine the error between the measurements and the simulation results, three different
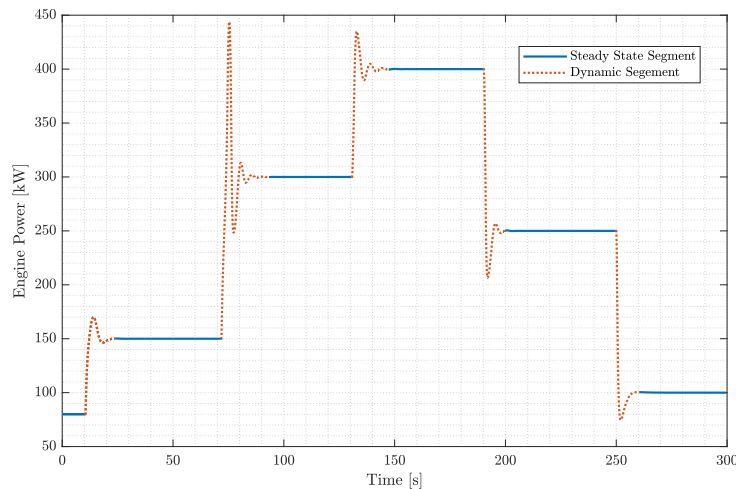


Figure 3: Engine power time trace showing the steady state and dynamic segments

indexes of performance [22, 13] have been evaluated for the complete validation run (Table 2), all steady state segments (Table 3) and all dynamic segments (Table 4). These indexes are defined as follows:

1. The mean absolute error (MAE):

$$\text{MAE}(h) = \frac{1}{m} \sum_{i=1}^{m} \left[ h(x_i^t) - y_i^t \right], \tag{10}$$

with $m$ the sample size, $h(x_i^t)$ the predicted model outcome for any given variable and for every sample point, and $y_i^t$ the measurement of the given variable;

2. The Mean Absolute Percentage Error (MAPE):

$$\text{MAPE}(h) = \frac{100}{m} \sum_{i=1}^{m} \left[ \frac{h(x_i^t) - y_i^t}{y_i^t} \right]; \tag{11}$$

3. The Pearson Product-Moment Correlation Coefficient (PPMCC):

$$\text{PPMCC}(h) = \frac{\sum_{i=1}^{m}(y_i^t - \bar{y})[h(x_i^t) - \hat{\bar{y}}]}{\sqrt{\sum_{i=1}^{m}(y_i^t - \bar{y})^2}\,\sqrt{\sum_{i=1}^{m}[h(x_i^t) - \hat{\bar{y}}]^2}}, \tag{12}$$

with $\bar{y} = \frac{1}{m}\sum_{i=1}^{m} y_i^t$ and $\hat{\bar{y}} = \frac{1}{m}\sum_{i=1}^{m} h(x_i^t)$.

The simulation was executed for validation using the Runge-Kutta method and a fixed step-size of 0.1 ms. This increased the computational costs significantly (execution time of 240 s), but the fixed step size ensured the correct ratio of sample points taken during the steady state and dynamic segments. For optimal performance, the simulation can be executed using a solver with a variable step size, which will increase the step size during steady-state segments. Using the Dormand-Prince method and a variable step size with a maximum step size of 0.1 s resulted in an execution time of 7 s. The simulation results of the validation have been obtained with MATLAB Simulink $R2023b$ running on an Intel Core $i7-1365U$ processor and 16 GB RAM.

Table 2: Performance measures complete simulation

| Variable | MAE | MAPE | PPMCC |
|---|---|---|---|
| Engine Power $P_b$ | 5.55 [kW] | 2.41 [%] | 0.9873 |
| Engine Speed $n_{eng}$ | 3.77 [rpm] | 0.25 [%] | 0.7370 |
| Throttle valve set point $THR_{set}$ | 2.93[%] | 10.76 [%] | 0.9127 |
| Turbocharger Speed $n_{TC}$ | 2277 [rpm] | 4.68 [%] | 0.9880 |
| Pressure air cooler $p_{ac}$ | 3.44 [kPa] | 2.38 [%] | 0.9882 |
| Pressure inlet receiver $p_{ir}$ | 3.07 [kPa] | 2.84 [%] | 0.9902 |
| Pressure outlet receiver $p_{or}$ | 4.27 [kPa] | 2.76 [%] | 0.9880 |
| Total engine efficiency $\eta_{eng}$ | 1.99[%] | 6.97 [%] | 0.8915 |

Table 3: Performance measures steady state segments

| Variable | MAE | MAPE | PPMCC |
|---|---|---|---|
| Engine Power $P_b$ | 1.06 [kW] | 0.62 [%] | 0.9999 |
| Engine Speed $n_{eng}$ | 0.77 [rpm] | 0.05 [%] | 0.0639 |
| Throttle valve set point $THR_{set}$ | 2.01[%] | 4.43 [%] | 0.9748 |
| Turbocharger Speed $n_{TC}$ | 1893 [rpm] | 4.21 [%] | 0.9965 |
| Pressure air cooler $p_{ac}$ | 2.54 [kPa] | 1.88 [%] | 0.9993 |
| Pressure inlet receiver $p_{ir}$ | 1.85 [kPa] | 1.96 [%] | 0.9988 |
| Pressure outlet receiver $p_{or}$ | 3.44 [kPa] | 2.24 [%] | 0.9990 |
| Total engine efficiency $\eta_{eng}$ | 1.69[%] | 6.21 [%] | 0.9977 |

Table 4: Performance measures dynamic segments

| Variable | MAE | MAPE | PPMCC |
|---|---|---|---|
| Engine Power $P_b$ | 19.40 [kW] | 7.77 [%] | 0.9487 |
| Engine Speed $n_{eng}$ | 12.99 [rpm] | 0.87 [%] | 0.7401 |
| Throttle valve set point $THR_{set}$ | 5.83[%] | 30.59 [%] | 0.8385 |
| Turbocharger Speed $n_{TC}$ | 3573 [rpm] | 6.48 [%] | 0.9592 |
| Pressure air cooler $p_{ac}$ | 6.33 [kPa] | 4.05 [%] | 0.9547 |
| Pressure inlet receiver $p_{ir}$ | 6.75 [kPa] | 5.57 [%] | 0.9642 |
| Pressure outlet receiver $p_{or}$ | 6.83 [kPa] | 4.35 [%] | 0.9549 |
| Total engine efficiency $\eta_{eng}$ | 2.89[%] | 9.24 [%] | 0.6163 |

### 3.2 Generator Step Load

The first use case examined represents the switching on of a large electrical consumer on the vessel's grid. For this use case, the engine model of the Caterpillar 3508$A$ gas engine is considered to be driving an electric generator

at a constant speed of 1500 rpm. Due to the switching, the generator load is increased instantaneously from 200 kW to 385 kW (40% to 77% of MCR). Consequently, the engine speed drops to 1415 rpm and fails the NATO STANAG 1008 for Quality Power Supply (QPS) by exceeding the worst case excursion for the grid frequency, see Table 5 and Figure 4.

The hybrid turbocharger's PTI function adds electric energy to the turbocharger shaft to improve the engine's step load response. Electric energy is added from the moment the generator load is increased and is held constant until the engine speed has stabilized (about 15 s after the load step). Different power settings for the PTI have been investigated, and the results for the inlet receiver pressure and the resulting engine speed are presented in Figure 4. With higher PTI power settings, the turbocharger shaft achieves higher acceleration rates and a faster compressor outlet pressure rise is realized, thus affecting the inlet receiver pressure. Due to the higher inlet receiver pressure, more air and fuel are forced into the cylinder and the engine develops more torque faster. This results in a quicker recovery of the engine speed and a smaller deviation from the speed set point. By providing 5 kW of electric power (or 2.5 kW per TC), the engine can pass the STANAG 1008 worst case excursion criterion. Increasing the PTI setting to 20 kW (or 10 kW per TC), the engine is even able to pass the STANAG 1008 transient tolerance criterion. Since the engine speeds deviate less from the set point, the overshoot during the recovery is also significantly reduced. The results show that hybrid turbocharging can significantly improve the engine's response to a step load and improve the stability of the electrical grid as well.

Table 5: QPS Frequency characteristics according to STANAG 1008 [41]

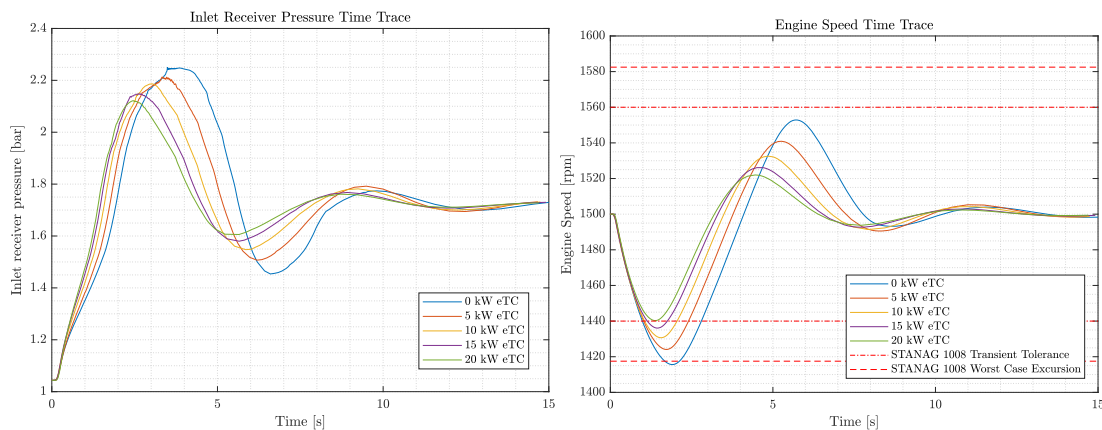| Characteristics | Tolerance | Transient Tolerance | Worst Case Excursion |
|---|---|---|---|
| Frequency $60Hz$ | ±3% | ±4% | ±5.5% |
| Recovery time | - | 2 s | 2 s |



Figure 4: Simulation results of inlet receiver pressure(left) and engine speed (right) for a step load 200 kW-385 kW and different PTI power settings

### 3.3 Case Vessel

For the second case study a typical CODOG propulsion plant of a fast naval combatant is considered, see Figure 5. Due to redundancy requirements, these propulsion plants consist of two independent shaft lines and at least one prime mover per shaft line. CODOG propulsion plants are always combined with controllable pitch propellers to facilitate easy reversing and improve the vessel's maneuverability. With this layout, the vessel can sail at cruise speed using reciprocating engines, and higher speeds are achieved by switching to the gas turbine. Since this paper focuses on the performance of reciprocating engines, gas turbines are not included in this research, and only ship speeds up to cruise speed are considered. Currently, no marine spark-ignited internal combustion engines are available, delivering sufficient power for this case study. Therefore, the Caterpillar 3508A gas engine, as presented in Table 1, is implemented. To match the requested torque at cruise speed, the engine's torque delivery is scaled by a factor 10 while all other engine parameters are held constant. The parameters of the case vessel are presented in Table 6.
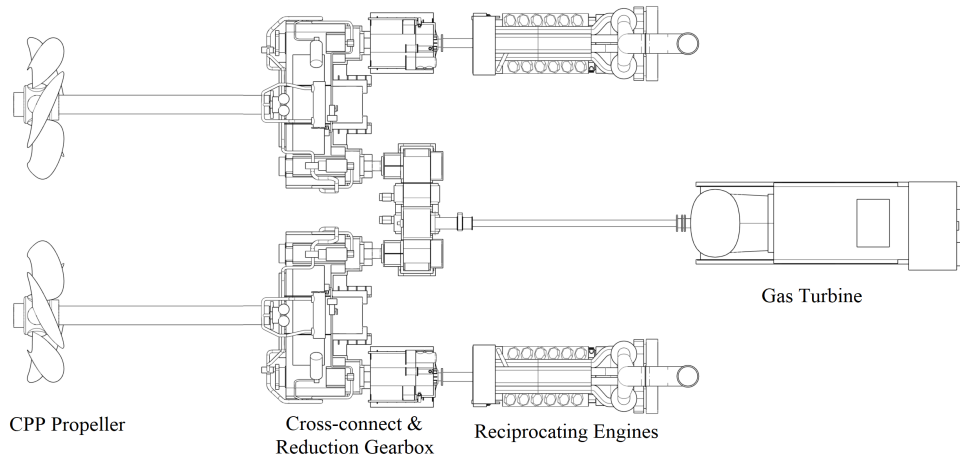
Figure 5: CODOG Propulsion System Layout

Table 6: Case vessel parameters, according to[53]

| Feature | Value |
|---|---|
| Ship mass $m_{ship}$ | $6000 \times 10^3$ [kg] |
| Design speed $v_{ship,d}$ | 28.7 [kn] |
| Total resistance at design speed $R_{ship,d}$ | 1309 [kN] |
| Number of propellers $k_p$ | 2 |
| Thrust deduction factor $f_t$ | 0.068 |
| Wake fraction $f_w$ | 0.05 |
| Propeller diameter $D_p$ | 4.8 [m] |
| Propeller pitch at design speed $PD_d$ | 1.8 |
| Gearbox reduction ratio cruise speed $i_{GB}$ | 14.563 |

### 3.4 Vessel Acceleration Manoeuvre

Due to the controllable pitch propellers, the vessel's achievable acceleration rate depends on the combination of propeller pitch and engine speed set points. The resulting combinator curve and the corresponding propeller pitch and engine speed increase rates are determined during the vessel's detailed design phase. They are often a trade-off between engine characteristics, propeller characteristics (mainly cavitation) and operational experiences.

Within this paper, two different approaches are implemented and investigated, presented in Figure 6. The first approach resembles the combinator curve typically implemented in the Royal Netherlands Navy (RNLN) frigates. With this approach, the propeller pitch is increased faster than the engine speed, resulting in a higher engine load and lower acceleration rate, see Figure 7. The second approach resembles the combinator curve implemented in the Royal Danish Navy's (RDN) air-defence (Iver Huitfeldt class) frigate. This frigate is propelled by four MTU 20V8000 engines in a CODAD propulsion plant arrangement. By increasing the engine speed early and faster than the propeller pitch, a higher acceleration rate is achieved by reducing the engine loading at the same time, see Figure 8. In combination with an adaptive pitch control strategy, propeller blade loading and resulting cavitation can be reduced while improving manoeuvrability [18].

To improve acceleration performance, the hybrid turbocharger's PTI function adds electric energy to the turbocharger shaft during the acceleration manoeuvre. For the acceleration manoeuvre, two cases are investigated: PTI with 200 kW per engine (or 100 kW per turbocharger) and PTI with 400 kW per engine (or 200 kW per turbocharger). With this additional power, the turbocharger's rotational speed increases, resulting in increased compressor outlet pressure. Depending on the throttle valve position, the increased compressor outlet pressure raises the inlet receiver pressure as well, resulting in a higher trapped mass of air in the cylinder. Ultimately, this results in an increased engine power limit, as shown in Figure 7 and Figure 8. For low compressor mass flows, corresponding with low engine speeds and low engine loads, the additional power provided via PTI has to be limited to prevent compressor surge, as discussed by Mestemaker et al. [39]. An excessive increase in the turbocharger speed due to high PTI settings will result in a quick rise in the compressor outlet pressure since the compressor mass flow is determined by the engine's swallow capacity, and flow separation in the compressor may occur. Higher compressor mass flows correspond with higher engine speeds and higher engine loads, reducing the risk of compressor

surge due to the greater margin between the compressor working point and the surge limit. Unfortunately, with high compressor mass flows, the effect of providing additional power via PTI on the compressor outlet pressure is diminished due to the high compressor power requested. As a result, the engine can only fully benefit from hybrid turbocharging if the engine is highly loaded while accelerating from medium to high engine speeds.

Results for the acceleration manoeuvre with the RNLN combinator approach, Figure 7, show that the propulsion engines benefit from the PTI and can deliver more power during the second half of the acceleration manoeuvre. The time needed to accelerate from 0 kn to 19 kn is reduced by 15 s (or about 10%) for a PTI setting of 200 kW per engine. Since the compressor outlet pressure does not linearly increase with the addition of electrical power via PTI, doubling of the PTI setting to 400 kW per engine results in just a slight increase in available engine power. The time needed to accelerate from 0 to 19 knots is reduced by an additional 5 s.

Results for the RDN combinator approach, Figure 8, show that in this situation, the propulsion engines only marginally benefit from hybrid turbocharging. By quickly ramping up the engine's speed with reduced propeller pitch, the requested power is limited, and the PTI's addition of energy is bound by the compressor surge limit. During the second half of the acceleration manoeuvre, the engine is running at maximum engine speed and providing additional power via PTI results in just a slight increase of the compressor outlet pressure. By implementing hybrid turbocharging, just a few seconds can be gained during the acceleration from 0 kn to 19 kn. Nevertheless, the RDN combinator approach without PTI results in a quicker acceleration manoeuvre than the RNLN combinator approach with the assistance of the hybrid turbocharger.

The results show that, depending on the design of the combinator curve, the propulsion engines can benefit from hybrid turbocharging during an acceleration manoeuvre. However, careful design of the combinator curve with respect to the engine envelope or adaptive pitch control strategies can facilitate higher acceleration rates than implementing hybrid turbocharging alone.
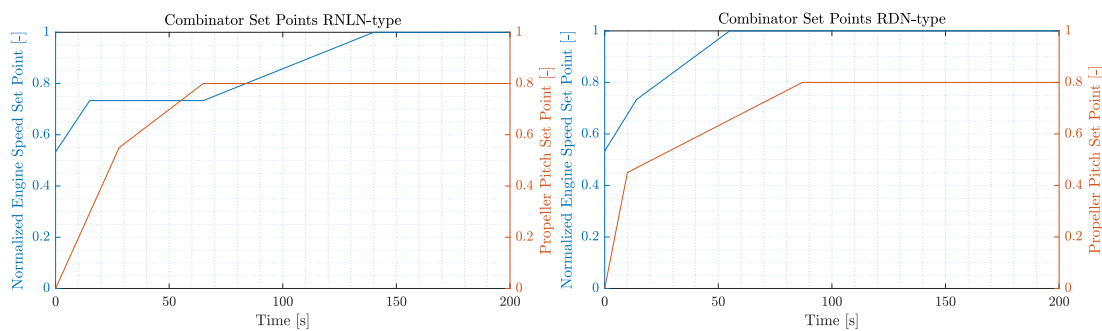


Figure 6: Combinator Set Points for Engine Speed and Propeller Pitch as used by the Royal Netherlands Navy (RNLN,left) and the Royal Danish Navy (RDN,right)



Figure 7: Results for the acceleration manoeuvre with the RNLN approach, showing the ship speed (left) and the requested power plotted in the engine envelope (right) for different PTI settings

## 3.5 Efficiency Considerations

The previous sections show that hybrid turbocharging can be beneficial for transient performances if additional electrical energy is fed to the turbocharger shafts. This electric energy has to be produced on board the vessel and is not freely available. Increasing the charge air pressure of the engine, either during a load step on the generator or
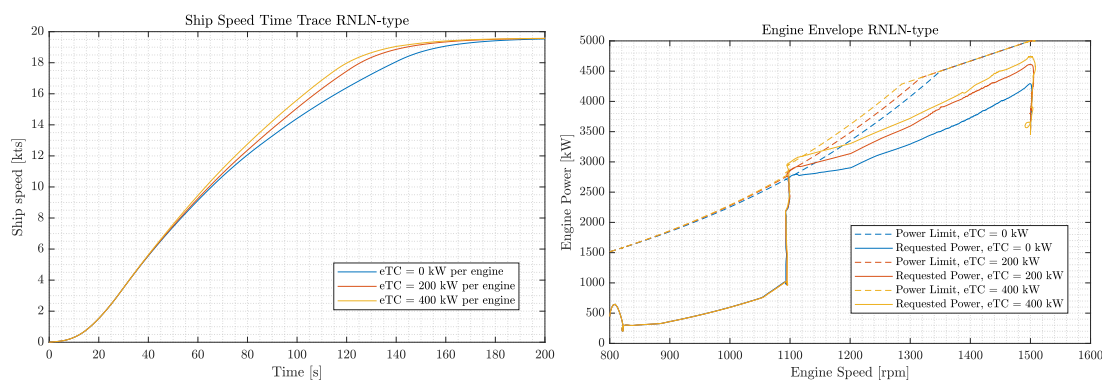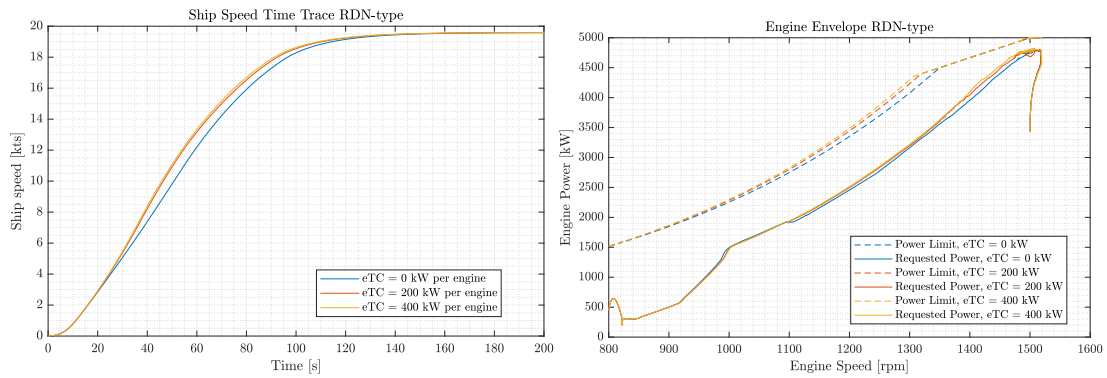
Figure 8: Results for the acceleration manoeuvre with the RDN approach, showing the ship speed (left) and the requested power plotted in the engine envelope (right) for different PTI settings

during an acceleration manoeuvre, can increase the engine's power output, supplying more fuel at the same time. Since the electric energy fed to the hybrid turbocharger cannot be recovered, total system efficiency decreases. Fortunately, transient phases, such as maneuvering, switching large electrical consumers, or starting up another generator set, represent a negligible part of a naval vessel's operational profile.

Considering the total system efficiency, it is thus more interesting to investigate steady state performance of the vessel. Using the PTO functionality of the hybrid turbocharger, electric energy can be subtracted from the shaft. Consequently, the compressor speed and resulting compressor outlet pressure are reduced. Unless the engine is running at maximum power and the throttle is fully opened, the charge air pressure (pressure in the inlet receiver) is held constant by the throttle valve by varying the throttle position and the resulting pressure difference across the throttle. Increasing the amount of electric energy subtracted with the hybrid turbocharger increases the throttle valve position. Essentially, the pumping losses of the engine are decreased while keeping the break power and thus the mechanical efficiency of the engine constant, see also Table 7 for the a ship speed of 20 kn. With this engine load, a maximum of 500 kW of electric power could be subtracted from the hybrid turbocharger, representing 10% of the nominal engine power.

Table 7: Throttle position and pressure values for different PTO settings on the propulsion engines at a ship speed of 20 kn

| PTO set point | 0 kW | 100 kW | 200 kW | 300 kW | 400 kW | 500 kW |
|---|---|---|---|---|---|---|
| **Throttle position** | 52.3° | 57.5° | 59.4° | 60.6° | 61.6° | 62.0° |
| **Turbocharger speed** | 77 600 rpm | 77 100 rpm | 76 200 rpm | 75 500 rpm | 75 200 rpm | 75 100 rpm |
| **Pressure compressor out** | 1.873 bar | 1.859 bar | 1.833 bar | 1.815 bar | 1.804 bar | 1.798 bar |
| **Pressure inlet receiver** | 1.640 bar | | | | | |
| **Engine Power** | 3650 kW | | | | | |

Since the PTO function of these propulsion engines is insufficient to cover the typical hotel load and provide backup capability for a naval combatant, additional generator sets are required. For the case vessel a hotel load of 2000 kW is considered and electric power is provided by two MTU 16V4000 diesel generator sets. With this configuration, four different scenarios are investigated, and the resulting system efficiency breakdown is presented in Table 8. The propulsion engines without PTO function and two running generator sets for electric power are considered in scenario 1. In the second scenario, the PTO function is designated as emergency power generation, and just one generator set is running to cover the hotel load. Since a maximum of 500 kW can be subtracted per propulsion engine, not the complete hotel load can be covered in case the generator set fails. However, 1000 kW should be sufficient to provide energy to all critical consumers and prevent a black-out. In scenarios 3 and 4, the PTO provides electric power, reducing the load on the two running generator sets. While subtracting a maximum of 500 kW per engine is possible, this results in increased sensitivity to external disturbances like wave loading and possible thermal overloading.

The results show that throttle-valve-controlled spark-ignited marine internal combustion engines achieve lower efficiencies compared to modern diesel engines due to significant throttling losses, especially in part load. However, these engines profit notably from hybrid turbocharging with the PTO function reducing throttling losses, resulting in an increase of the engine efficiency of up to 4% during cruise speed of 20 kn. The gain in engine efficiency of the propulsion engines even offsets the declining engine efficiency of the diesel generators, thus resulting in an

Table 8: System efficiency breakdown, ship speed 20 kn, hotel load 2000 kW

|  | **Without PTO** | **PTO standby** | **PTO** 250 kW | **PTO** 500 kW |
|---|---|---|---|---|
| **Propulsion engine load** | 3650 kW | 3650 kW | 3650 kW | 3650 kW |
| **PTO** | 0 kW | 0 kW | 250 kW | 500 kW |
| **Propulsion engine efficiency** | 0.297 | 0.297 | 0.318 | 0.338 |
| **Number of gensets running** | 2 | 1 | 2 | 2 |
| **Genset load** | 1000 kW | 2000 kW | 750 kW | 500 kW |
| **Genset efficiency** | 0.38 | 0.41 | 0.34 | 0.32 |
| **System efficiency** | 0.311 | 0.316 | 0.321 | 0.335 |

increase in the propulsion system's total efficiency.

## 4 Conclusions and Future Work

This paper has explained how hybrid turbocharging can benefit marine spark-ignited combustion engines running on alternative fuel. An existing Mean Value First Principle (MVFP) model has been extended and validated to investigate hybrid turbocharging. For validation, we introduced three different performance indexes and presented their results for the steady state and dynamic segments of the simulation run. We can conclude from the validation that a mean value simulation model can perform with reasonable accuracy and predict the gas path dynamics well enough to investigate the effects of hybrid turbocharging on transient performance.

By investigating different use cases, the effect of hybrid turbocharging during transient phases and steady state has been evaluated. We have shown how the response of a marine generator set running on alternative fuel to a load change can be improved by using the hybrid turbocharger's PTI function. A hybrid turbocharger can significantly reduce the engine speed drop after a load step, thus increasing the grid's stability. This allows for larger load steps while complying with NATO STANAG 1008. For spark-ignited propulsion engines running on alternative fuels, we can conclude that the advantages of a hybrid turbocharger are limited during an acceleration manoeuvre. Although the time required to accelerate from 0 to cruising speed can be reduced slightly using the hybrid turbocharger's PTI function, larger performance gains can be achieved with propeller pitch and engine speed set points that match the engine's envelope. This stresses again the importance of a well designed combinator curve to improve maneuverability and reduce time. However, implementing hybrid turbocharger on the propulsion engines can improve the system efficiency with 2.5% during steady state phases. Using the PTO function reduces throttling losses, and the additional electric power is fed to the vessel's grid.

Special attention was paid to preventing compressor surging while simulating the acceleration manoeuvre with PTI on the hybrid turbocharger. At low to medium engine speeds, the margin between the normal operating point and compressor surge is very small. Future work should include blow-off, blow-by, and waste gate valves as well as considering alternative compressor and turbine sizing to increase the charge air pressure at low engine speeds without exceeding the surge limit. With these extensions in mind, different maneuvering operations should be investigated, including acceleration with varying initial ship speeds and sea margins. Furthermore, additional steady state cases should be investigated, including the effects of PTO and PTI with varying engine load and external disturbances. Although the current model can predict the performance and efficiency of the investigated gas engine within reasonable accuracy, extending the gas path might require a more sophisticated simulation approach since not all aspects of blow-off, blow-by and waste gate control can be captured well with a mean value model.

## Acknowledgement

## References

[1] Aghaali, H., Angström, H.E., 2015. A review of turbocompounding as a waste heat recovery system for internal combustion engines. Renewable and sustainable energy reviews 49, 813–824.

[2] Altosole, M., Balsamo, F., Campora, U., Mocerino, L., 2021. Marine dual-fuel engines power smart management by hybrid turbocharging systems. Journal of Marine Science and Engineering 9, 663.

[3] Altosole, M., Benvenuto, G., Campora, U., Silvestro, F., Terlizzi, G., 2018. Efficiency improvement of a natural gas marine engine using a hybrid turbocharger. Energies 11, 1924.

[4] Baines, N., 2005. Fundamentals of Turbocharging. Concepts NREC.

[5] Bilousov, I., Bulgakov, M., Savchuk, V., 2020. Modern Marine Internal Combustion Engines. Springer.

[6] Boretti, A., 2018. Changes of e-kers rules to make f1 more relevant to road cars. Advances in Technology Innovation 3, 26.

[7] Bosklopper, J., Sapra, H., van de Ketterij, R., van Sluijs, W., Bekdemir, C., de Vos, P., Visser, K., 2020. Experimental study on a retrofitted marine size spark-ignition engine running on port-injected 100% methanol. INEC 2020, Delft .

[8] Breitbach, H., Christmann, R., Gabriel, H., Metz, D., 2020. Die zweite generation des ebooster von borgwarner. MTZ-Motortechnische Zeitschrift 81, 46–49.

[9] Bricknell, D.J., Partridge, R., 2006. Power and propulsion for the modern global combatant. Horizon 124, F100.

[10] Bucknall, R., Suarez De La Fuente, S., Szymko, S., Bowers, W., Sim, A., 2018. Evaluation of electric-turbo-charging applied to marine diesel-engines, in: Conference Proceedings of INEC, pp. 1–12.

[11] Campora, U., Coppola, T., Micoli, L., Mocerino, L., Ruggiero, V., 2023. Techno-economic comparison of dual-fuel marine engine waste energy recovery systems. Journal of Marine Science and Application 22, 809–822.

[12] Casson, C.P., Wood, C.J., Bricknell, D.J., Daffey, K., Partridge, R., 2006. Power and propulsion for the new global combatant. Brycheins Ltd. .

[13] Coraddu, A., Oneto, L., Cipollini, F., Kalikatzarakis, M., Meijn, G.J., Geertsma, R., 2022. Physical, data-driven and hybrid approaches to model engine exhaust gas temperatures in operational conditions. Ships and Offshore Structures 17, 1360–1381.

[14] Cross, D., Brockbank, C., 2009. Mechanical hybrid system comprising a flywheel and CVT for motorsport and mainstream automotive applications. Technical Report. SAE Technical Paper.

[15] Dang, J., Van den Boom, H., Ligtelijn, J.T., 2013. The wageningen c-and d-series propellers, in: 12th International Conference on Fast Sea Transportation FAST, Citeseer. pp. 1–10.

[16] Dang, J., Brouwer, J., Bosman, R., Pouw, C., 2012. Quasi-steady two-quadrant open water tests for the wageningen propeller c-and d-series, in: Proceedings of the Twenty-Ninth Symposium on Naval Hydrodynamics, Gothenburg, Sweden, pp. 1–19.

[17] Davies, P., Bontemps, N., Tietze, T., Faulseit, E.T., 2019. Elektrisch unterstützte turboaufladung-schlüsseltechnologie für hybridisierte antriebsstränge. MTZ-Motortechnische Zeitschrift 80, 30–39.

[18] Drakoulas, M., Reurings, J., Meijn, G., Wittingen, M., 2022. Adaptive pitch control: Simulation performance evaluation against conventional propulsion control, in: Conference Proceedings of INEC, pp. 1–13.

[19] Ekberg, K., Eriksson, L., 2017. Improving fuel economy and acceleration by electric turbocharger control for heavy duty long haulage. IFAC-PapersOnLine 50, 11052–11057.

[20] Figari, M., Theotokatos, G., Coraddu, A., Stoumpos, S., Mondella, T., 2022. Parametric investigation and optimal selection of the hybrid turbocharger system for a large marine four-stroke dual-fuel engine. Applied Thermal Engineering 208, 117991.

[21] Geertsma, R., Negenborn, R., Visser, K., Loonstijn, M., Hopman, J., 2017. Pitch control for ships with diesel mechanical and hybrid propulsion: Modelling, validation and performance quantification. Applied energy 206, 1609–1631.

[22] Ghelardoni, L., Ghio, A., Anguita, D., 2013. Energy load forecasting using empirical mode decomposition and support vector regression. IEEE Transactions on Smart Grid 4, 549–556.

[23] Golloch, R., Merker, G.P., 2005. Downsizing bei verbrennungsmotoren. MTZ-Motortechnische Zeitschrift 66, 126–131.

[24] Heiduk, T., Weiß, U., Fröhlich, A., Helbig, J., 2016. Der neue v8-tdi-motor von audi teil 1: Aggregatearchitektur und aufladekonzept mit elektrischem verdichter. MTZ-Motortechnische Zeitschrift 77, 24–31.

[25] Heim, K., 2002. Existing and future demands on the turbocharging of modern large two-stroke diesel engines, in: 8-th Supercharging Conference, Dresden, pp. 1–2.

[26] Herring, P., 1987. Sequential turbocharging of the mtu 1163 engine. Transactions 100.

[27] Heywood, J.B., 1988. Internal combustion engine fundamentals. Mcgraw-hill.

[28] Hiereth, H., Prenninger, P., 2007. Charging the internal combustion engine. Springer Science & Business Media.

[29] Hoang, A.T., Foley, A.M., Nižetić, S., Huang, Z., Ong, H.C., Ölçer, A.I., Nguyen, X.P., et al., 2022. Energy-related approach for reduction of co2 emissions: A critical strategy on the port-to-ship pathway. Journal of Cleaner Production 355, 131772.

[30] Hopmann, U., Algrain, M.C., 2003. Diesel engine electric turbo compound technology. Technical Report. SAE Technical Paper.

[31] Hountalas, D., Katsanos, C., Lamaris, V., 2007. Recovering energy from the diesel engine exhaust using mechanical and electrical turbocompounding. Technical Report. SAE Technical Paper.

[32] Inal, O.B., Charpentier, J.F., Deniz, C., 2022. Hybrid power and propulsion systems for ships: Current status and future challenges. Renewable and Sustainable Energy Reviews 156, 111965.

[33] Katrašnik, T., Trenc, F., Medica, V., Markič, S., 2005. An analysis of turbocharged diesel engine dynamic response improvement by electric assisting systems. Journal of Engineering for Gas Turbines and Power .

[34] Kech, J., Hegner, R., Mannle, T., 2014. Turbocharging: Key technology for high-performance engines. MTU Engine Technology White Paper .

[35] Kech, J., Rappsilber, R., Thiesemann, J., 2019. Elektrisch unterstützte aufladung für off-highway-hochleistungsmotoren. MTZ-Motortechnische Zeitschrift 80, 52–61.

[36] Kisbenedek, E., Andersson, N., 2018. Review on Recent Advances for Marine Turbocharger Technologies. B.S. thesis. CHALMERS UNIVERSITY OF TECHNOLOGY.

[37] Mack Trucks, 2020. Mack announces updated mp8he engine with turbocompounding. https://dieselnet.com/news/2020/10mack.php. Accessed: 2024-04-29.

[38] McKinlay, C.J., Turnock, S.R., Hudson, D.A., 2021. Route to zero emission shipping: Hydrogen, ammonia or methanol? International journal of hydrogen energy 46, 28282–28297.

[39] Mestemaker, B., Westhoeve, J., Visser, K., 2019. Evaluation of hybrid electric turbocharging for medium speed engines. Technical Report. SAE Technical Paper.

[40] Montal Almirall, D., 2019. Electric power generation from the hybrid turbocharger of a marine propulsion diesel engine. B.S. thesis. Universitat Politècnica de Catalunya.

[41] NATO, 2021. NATO - STANAG 1008: CHARACTERISTICS OF SHIPBOARD 440V/230V/115V 60Hz, 440V/115V 400Hz and 24/28VDC ELECTRICAL POWER SYSTEMS IN WARSHIPS OF THE NATO NAVIES. Technical Report. North Atlantic Treaty Organization (NATO).

[42] Nielsen, J.B., Yum, K.K., Pedersen, E., 2020. Improving pre-turbine selective catalytic reduction systems in marine two-stroke diesel engines using hybrid turbocharging: A numerical study of selective catalytic reduction operation range and system fuel efficiency. Proceedings of the Institution of Mechanical Engineers, Part M: Journal of Engineering for the Maritime Environment 234, 463–474.

[43] Pasini, G., Lutzemberger, G., Frigo, S., Marelli, S., Ceraolo, M., Gentili, R., Capobianco, M., 2016. Evaluation of an electric turbo compound system for si engines: A numerical approach. Applied Energy 162, 527–540.

[44] Piancastelli, L., Peli, F., Pezzuti, E., et al., 2018. The advantage of the "split" turbocharger in formula 1 engines. Tecnica Italiana 61, 36–41.

[45] Pucher, H., Zinner, K., 2012. Aufladung von Verbrennungsmotoren: Grundlagen, Berechnungen, Ausführungen. Springer-Verlag.

[46] Rusman, J., 2018a. Charge air configurations for propulsion diesel engines aboard fast naval combatants, in: Conference Proceedings of INEC, pp. 1–11.

[47] Rusman, J., 2018b. Charge air configurations for propulsion diesel engines aboard fast naval combatants. Msc thesis. Delft UNIVERSITY OF TECHNOLOGY.

[48] Sapra, H., Linden, Y., van Sluijs, W., Godjevac, M., Visser, K., 2019. Experimental investigations of performance variations in marine hydrogen-natural gas engines, in: Cimac Congress, pp. 1–17.

[49] Saunders, S., 2015. Jane's Fighting Ships 2015-2016. Janes.

[50] Scheub, J., Zecchetti, D., Habermann, J., Maniar, M., 2021. Mehr effizienz und leistung mittels elektrischem turbolader. MTZ-Motortechnische Zeitschrift 82, 78–84.

[51] Schmalzl, H.P., 2014. Zurück in die zukunft wege der aufladung. MTZ-Motortechnische Zeitschrift 75, 90–95.

[52] Shiraishi, K., Krishnan, V., 2014. Electro-assist turbo for marine turbocharged diesel engines, in: Turbo Expo: Power for Land, Sea, and Air, American Society of Mechanical Engineers. p. V01BT23A003.

[53] Vollbrandt, J., 2016. Improving the maneuvering performance of diesel hybrid propulsion plants for fast naval combatant. Msc thesis. Delft UNIVERSITY OF TECHNOLOGY.

[54] Vollbrandt, J., Coraddu, A., Geertsma, R., 2023. Transient performance of alternatively fueled internal combustion engines for naval applications, in: Conference Proceedings of EAAW, pp. 1–11.

[55] Volvo Group, 2021. With continued north american success, volvo truck's d13 turbo compound engine now standard on all vnl models. https://www.volvogroup.com. Accessed: 2024-04-29.

[56] Watson, N., Janota, M.S., 1982. Turbocharging the internal combustion engine. Macmillan Education UK.

[57] Webster, J.S., Fireman, H., Allen, D.A., Mackenna, A.J., Hootman, J.C., 2007. Us navy studies on alternative fuel sources and power and propulsion methods for surface combatants and amphibious warfare ships. Naval engineers journal 119, 35–48.

[58] Westhoeve, J., 2018. Hybrid Electric Turbocharging: Improving the loading capability and efficiency of a dual fuel engine. Msc thesis. Delft UNIVERSITY OF TECHNOLOGY.

[59] Wilbur, C.T., Wight, D., 2016. Pounder's marine diesel engines. Elsevier.

[60] Woodyard, D., 2009. Pounder's marine diesel engines and gas turbines. Butterworth-Heinemann.

[61] Woud, J.K., Stapersma, D., 2002. Design of propulsion and electric power generation systems. IMarEST.

[62] Zellbeck, H., Friedrich, J., Berger, C., 1999. Die elektrisch unterstützte abgasturboaufladung als neues aufladekonzept. MTZ-Motortechnische Zeitschrift 60, 386–391.